Available online at www.sciencedirect.com
SCIENCE DIRECT®
Journal of Nuclear Materials 337–339 (2005) 322–326
journal of nuclear materials
www.elsevier.com/locate/jnucmat

Velocity fields of edge/Scrape-Off-Layer turbulence in Alcator C-Mod

J.L. Terry [a,*], S.J. Zweben [b], O. Grulke [c], M.J. Greenwald [a], B. LaBombard [a]

[a] *Plasma Science and Fusion Center, Massachusetts Institute Technology, Room NW 17-176, 175 Albany Street, Cambridge, MA 02139, USA*
[b] *Princeton Plasma Physics Lab., Princeton, NJ, USA*
[c] *MPI for Plasma Physics, EURATOM Association, Greifswald, Germany*

Abstract

Using high speed movies of edge/Scrape-Off-Layer emission, velocity fields of the turbulent fluctuations have been measured in a small region of the poloidal/radial plane at the plasma's outboard midplane. Gas-puff-imaging is used to localize the emission in the toroidal dimension. The measured D_α line emission responds to the underlying spatio-temporal dynamics of density and temperature. Time-delay cross-correlation analysis is applied to the 64×64 pixel movie images and yields time-averaged velocity fields for the emission perturbations. The spatial resolution of the velocity determinations is a few mm over the viewed region. It is found that the velocities inside the separatrix are almost purely poloidal. In the SOL the radial velocity component is outward, and significant radial acceleration is observed. The poloidal and radial components of the SOL velocities vary with the discharge conditions. The magnitudes of all the velocity components measured this way range from 0 to $\sim$1000 m/s.

PACS: 52.35.R; 52.70; 52.55; 52.40.H
Keywords: Cross-field transport; Edge plasma; Fluctuations and turbulence; Intermittent transport; Visible imaging; Alcator-C-mod

1. Introduction

It has been known for some time that the edges of tokamak plasmas are turbulent. More recently, it has been shown that in the Scrape-Off-Layer (SOL) perpendicular particle transport competes with or dominates parallel transport along open field lines [1]. This high level of perpendicular transport has important consequences for characteristic 'Scrape-Off' lengths, for reactor divertor and first wall design, and for recycling. This cross-field particle transport is typically strongly intermittent and convective [2, and references therein]. It is primarily driven by the turbulence, with the larger amplitude events responsible for a large fraction of the transport [3]. Understanding of the turbulence and the enhanced transport that accompanies it is presently the goal of intense investigation. Both experiment [4] and modeling [5,6] indicate that the turbulence drive is ballooning-like. One of its common characteristics is the generation of 'filaments' of the density and potential perturbations that are field-aligned and have small $k_\parallel$. When these filaments are viewed in cross-section, i.e. parallel to the local magnetic field, they appear as

* Corresponding author. Tel.: +1 617 253 8637; fax: +1 617 253 0627.
E-mail address: terry@psfc.mit.edu (J.L. Terry).

0022-3115/$ - see front matter © 2004 Elsevier B.V. All rights reserved.
doi:10.1016/j.jnucmat.2004.10.092

clumps or 'blobs' and are evident as large amplitude I_{sat} or $V_{floating}$ events on probes. There is an extensive literature on 'blobs', e.g. [1–3] and on 'blob' propagation [7, and Refs. within]. Of particular interest is the generation and propagation of these filaments/blobs. The velocity fields reported here are strongly influenced by the blob propagation since they can dominate the perturbations whose dynamics are being represented. Thus this research is part of the effort to understand the anomalous turbulent transport. In particular, the measured velocity fields can be compared directly with models of both blob generation and propagation. We believe that these measurements have the highest 2D spatial resolution of any simultaneous many-point measurement to date.

Time sequences of 2D images ('movies') have been used extensively as plasma diagnostics for a long time; see e.g. [8]. As we report here, we are using 2D movies to study, for periods of ~1 ms, the edge turbulence in tokamaks that occurs on a $\gtrsim$10 μs timescale with a R, Z spatial scale of ~3–50 mm. We have used a special CCD-based 'ultra-fast' camera system [9] that is capable of recording three hundred, 64×64 pixel frames at a maximum 250 kHz frame rate. In deriving the velocity fields of the turbulent perturbations from the time sequences of images, we demonstrate the potential of this technique for studying the dynamics of the edge/SOL turbulence. There is also great potential for studying edge and *core* turbulence using arrays of 'single-channel' views [10] in combination with neutral beam injection.

2. 'Gas-puff imaging' of edge turbulence

We have set up the camera to view light emission from the outboard midplane of C-Mod. In addition to the intrinsic D_α emission from the plasma periphery, additional atoms are supplied by puffing D_2 through a 4-barrel nozzle that is located near the plasma edge. The local atom source results in toroidally localized emission that is viewed by in-vessel optics along sightlines parallel to the local magnetic field. If the local source is large enough, then the local emission dominates the intrinsic and results in a toroidally localized measurement. The technique is called 'gas-puff imaging' (GPI) and is described in greater detail in Refs. [11,12]. A ~6 cm × 6 cm diamond-shaped region of plasma edge/SOL in front of the nozzle is imaged onto a coherent fiber bundle, which brings the image to an interference filter and ultimately to the intensified camera. There is considerable fluctuation in measured emission, with the RMS levels (normalized by the time-average) exceeding 50% in some regions. The emission fluctuations are a result of the underlying turbulent fluctuations in plasma electron density and temperature, not the result of fluctuations in the atom density. Modeling of the atomic physics indicates that the D_α emission is proportional to $n_o \times n_e^\alpha \times T_e^\beta$, with $0.5 < \alpha < 0.8$ and $0.3 < \beta < 1.4$ [13,12]. Using the system described above, movies of edge/SOL turbulence, as manifested in the GPI emission, were recorded for 1.2 ms at a 250 kHz frame rate. The time-average emission pattern is 'windowed' radially by atomic physics, limited on the hot side by ionization and on the wall side by lack of excitation. The average emission typically straddles the separatrix and decreases somewhat at the top and bottom of the view, a result of the vertical distribution of atoms from the nozzles.

All of the camera movies show the intermittent birth and subsequent motion of isolated regions of strong emission. These are the blobs. The image sequences serve as the raw material for the analysis that yields the velocity fields that are the subject of this report.

3. Time-delay cross-correlation analysis of GPI movies and velocity fields

We analyze the movies by first removing the 'DC' component of the D_α emission pattern, i.e. the time-average of all 300 frames. The time-average image is subtracted from all individual images, yielding a movie of the fluctuations. Such a 'fluctuation' frame is shown in Fig. 1. A rectangular subsection of each diamond-shaped 64×64 pixel image is then selected. Its edges are aligned parallel to the radial and vertical directions in the tokamak geometry, and its extent is chosen based on the extent of useful time-averaged signal. A median filter is applied to the image to 'smooth' it over each

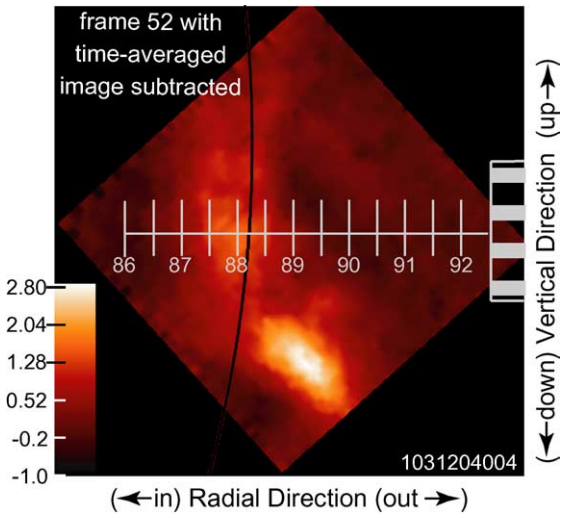

Fig. 1. One frame from the movie whose time-average has been subtracted. A 'blob' is seen near the bottom. This is feature is seen in the raw image as well. Also shown is the location of the magnetic separatrix (solid black line) and the nozzle through which the D_2 was puffed (at right).

$\sim 4 \times 4$ mm region. (The actual optical resolution is ~ 2 mm, and this choice of smoothing was not optimized.) Each 'smoothed' pixel's time history is then cross-correlated (for the entire 300 frame sample duration) with every other pixel's time history. Contours of cross-correlation values are thus generated. This is done for eight different lag times from –16 μs to +12 μs in 4 μs steps. The cross-correlation function between pixels i and j with time lag τ is defined (in the $\tau > 0$ case) as

$$C_{i,j}^{\tau} = \frac{\sum_l (I_i(t_l) - \bar{I}_i)(I_j(t_l + \tau) - \bar{I}_j)}{\sqrt{\sum_l (I_i(t_l) - \bar{I}_i)^2 \sum_l \left(I_j(t_l) - \bar{I}_j\right)^2}},$$

where $I_i(t_l)$ is the time series intensity from the ith pixel, and the numerator sum is over 300-(τ/4 μs) time points. At each lag time the spatial location of the cross-correlation maximum is found and the motion of this maximum is taken to be the *time-averaged* phase velocity of the perturbations/fluctuations at that point. All cross-correlation maxima are >0.55. Examples of the cross-correlation contour plots for a single R, Z location are shown for the first time-lag (−16 μs) and last time-lag (+12 μs) maxima in Fig. 2. Time-lag maxima are also calculated for the intermediate time-lags (−12 to +8 μs) in order to see the 'scatter' in velocities calculated from each pair of adjacent time-lag maxima. These are shown in the right panel of Fig. 2 as the line segments demarked by ♦s. This procedure is repeated over the smoothed pixel grid of the image rectangle, and the grid of velocity vectors is determined.

Fig. 3 shows a velocity field measured in the manner described above. It is measured in the steady-state portion of an L-mode ohmic discharge. The magnetic configuration is with a lower single null (LSN). Three things are evident. First, the velocities inside the separatrix (on the closed flux surfaces) are essentially purely poloidal and point downward. This is in the ion diamagnetic direction and corresponds to a positive E_r if the perturbation movement is dominated by $E_r \times B$ motion. Magnitudes are of order 500 m/s. Second, at the separatrix the velocities change direction abruptly. In this case the motion in the SOL is predominantly radially outward, with 500 m/s as the order of magnitude. Third, in the SOL there is a radial acceleration.

Since there is significant variation in the observed fields that is dependent upon discharge type, we present three other examples of the velocity field measurements. Shown in Fig. 4 is the perturbation velocity field from an

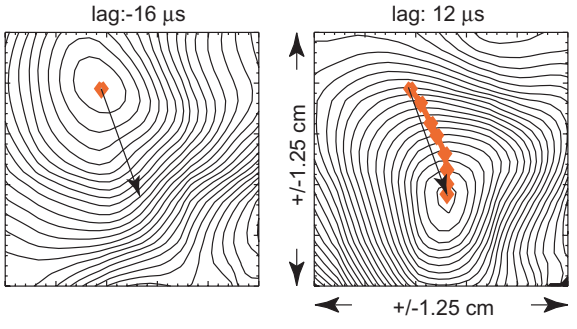

Fig. 2. Contour plots of cross-correlation values at time lags of –16 and +12 μs. The cross-correlation is done with the pixel at the center of the plotted region and is done over the entire time sample. The arrow indicates the velocity calculated for this location; the short segments linked by diamonds show progression the velocity segments between successive time lags.

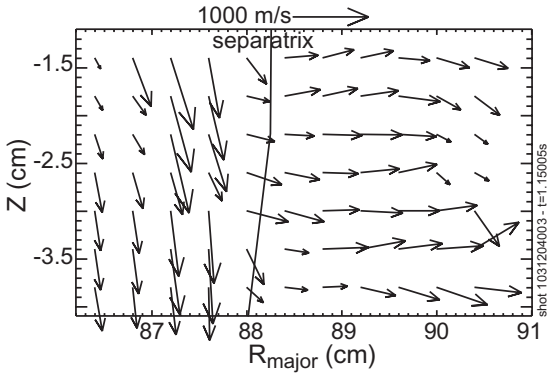

Fig. 3. Velocity field of perturbations for an L-mode LSN discharge. The lengths and directions of the arrows indicate the magnitude and direction of the velocities. The arrow above the figure has $[V_R, V_Z] = [1000, 0]$ m/s and calibrates the field arrows.

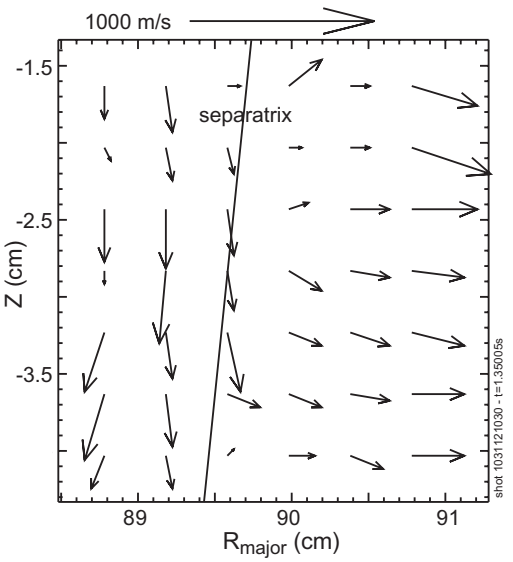

Fig. 4. Velocity field of perturbations for an ELMfree H-mode LSN discharge. The arrow above the figure has $[V_R, V_Z] = [1000, 0]$ m/s and calibrates the field arrows.

ELMfree H-mode (LSN) discharge. It has the same qualitative features that are seen in the L-mode case (Fig. 3). However, other discharges were observed to have quantitatively different features, in particular much larger poloidal velocity components in the SOL. Different fields are shown in Fig. 5, where fields from a LSN and an upper single null (USN) L-mode discharge are compared. These discharges were set up to be very similar in every respect except the X-pt location. It is seen that this affects the velocities, since in the USN case, Fig. 5(b), there are radial regions around $R \sim 90\,\mathrm{cm}$ where the poloidal velocity components are *upward*. This difference is reproducible since the same discharges were repeated five shots later, and similar fields were found. From these and similar observations we conclude that, although the fluctuation motion and the velocity fields derived from that motion are reproducible for similar shots, there is a variation that depends on a mechanism that is not as yet known. Certainly the confinement mode (L- or H-mode) is *not* enough to determine the fields, and the location of the null does affect the observed velocity fields.

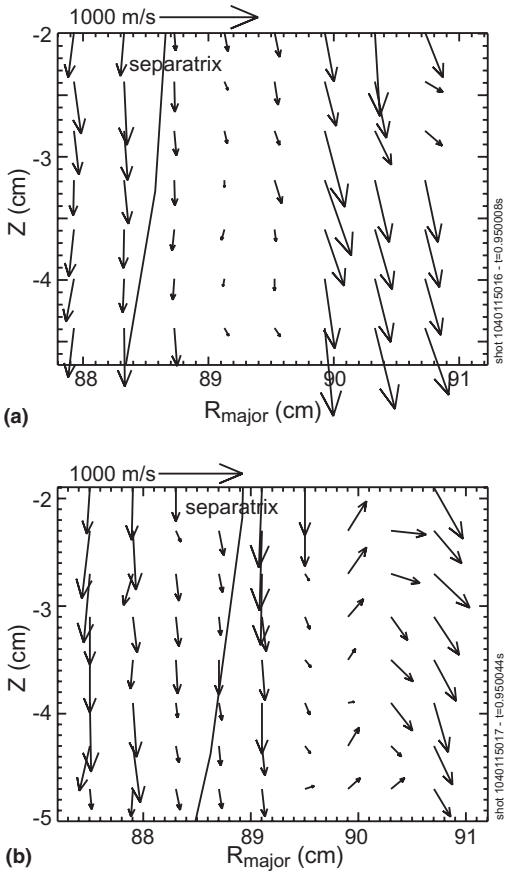

Fig. 5. (a) Velocity field of perturbations for an L-mode LSN discharge. (b) Velocity field of perturbations for an L-mode USN discharge that is otherwise very similar to that of (a). Note the region in the SOL of upward motion. The arrows above the figures have $[V_R, V_Z] = [1000, 0]\,\mathrm{m/s}$ and calibrate the field arrows.

4. Discussion and summary

It is important to note that what is calculated for the velocity field agrees with what is seen in the movies by the human observer. That is, intermittent 'blobs' similar to the one seen in Fig. 1 are born and move predominantly outward and/or downward in a way that is on average consistent with the derived fields. For example, in the USN case of Fig. 5(b), there is a mixture of 'blobs' moving both upward and downward, while for the cases shown in Figs. 3 and 4, the 'blob' motion is predominantly outward. Also in those cases with well defined 'blobs', the velocities found by tracking a given 'blob' agree approximately with the velocities of the cross-correlation analysis.

The picture *inside* the separatrix is less clear, since well defined 'blobs' (like that of Fig. 1) rarely occur there. Nonetheless, there are certainly fluctuations in this region that are tracked by the analysis. Inside the separatrix probe measurements show that typically the fluctuations move in the electron diamagnetic drift direction [14], i.e. *opposite* to what is seen here, with poloidal velocities $\sim 5\times$ higher than the $\sim$500–1000 m/s measured here. The reasons for the difference are presently unknown. Nonetheless, because of this striking difference, and because E_r is probably <0 just inside the separatrix (i.e. consistent with an *upward* $E \times B$ flow), we must examine the present result critically. The probe measurements of fluctuation phase velocities (shown in Fig. 3 of [14]) are based on fluctuations with $|k_{\mathrm{pol}}| \lesssim 5\,\mathrm{cm}^{-1}$. The present measurement is sensitive to $1\,\mathrm{cm}^{-1} \lesssim |k_{\mathrm{pol}}| \lesssim 15\,\mathrm{cm}^{-1}$. In addition, inside the separatrix the frequency spectra of individual pixels are above the noise floor only for $f \lesssim 20\,\mathrm{kHz}$, so the maximum phase velocity from the movie analysis that can be trusted is $\omega^{\max}/k_{\mathrm{pol}}^{\min} \sim 1300\,\mathrm{m/s}$. Actual phase velocities higher than this may alias the values determined using the movies analysis. Since the probe-based phase velocities inside the separatrix are typically 2–5 km/s, aliasing may be occurring in the movie analysis. It would be useful to make simultaneous measurements with both diagnostics at the same location, although this is not possible with the present diagnostic setup on C-mod.

Outside the separatrix, probe measurements typically show downward poloidal propagation, consistent with the dominant poloidal direction found in these analyses (at least in those cases where there is a significant poloidal component). The poloidal velocities are approximately consistent as well. The sharp change in the field distribution at the separatrix, as evidenced in Figs. 3

and 4, suggests that the division between open and closed field lines can play a key role, and appears to support some of the features of the 'blob' propagation models developed in Ref. [7] Finally, it worth considering what more can be done using the movies and this type of analysis. We have used the entire 300 frame sample in the cross-correlations. It may be possible to reduce this sample in the analysis to produce time-varying velocity fields. In addition, *if* the velocity measured is dominated by 'blob' propagation (as is likely in the far SOL) and *if* the 'blobs' carry plasma (which is also likely), then the time-average of the dot-product of the perturbation velocity field and the emission field could be calculated to yield a blob-driven 'flux'. In that case we would, to zeroth order, neglect the atomic physics of the emission process and take the emission field to be that of the plasma density and calculate $\langle \tilde{n}'' \cdot \tilde{V} \rangle$. This would then give a rough measure of blob flux, a quantity that would be quite valuable for the understanding of edge turbulence and transport.

In summary, we have described the use of a time-delay cross-correlation technique in the analysis of high speed movies of edge/SOL emission. By looking at the fluctuations about the time-averaged image, we have measured the poloidal and radial phase velocity fields of the turbulent perturbations. This has been done viewing a small region at the plasma's outboard midplane. Spatial resolution of a few mm in the velocity field has been demonstrated. It is found that the velocities inside the separatrix are almost purely poloidal with magnitudes from ~300–1000 m/s. In the SOL the radial velocity component is outward, and some radial acceleration is observed. The poloidal and radial components of the SOL velocities vary with the discharge conditions with magnitudes varying between 0 and ~1000 m/s.

Acknowledgments

This work is supported by DoE Coop. Agreement DE-FC02-99-ER54512 and Contract No. DE-AC02-76CHO3073.

References

[1] B. LaBombard et al., Nucl. Fus. 40 (2000) 2041.
[2] B. LaBombard et al., Phys. Plasmas 8 (2001) 2107; J.A. Boedo et al., Phys. Plasmas 8 (2001) 4826.
[3] D.L. Rudakov et al., Plasma Phys. Control. Fus. 44 (2002) 717.
[4] J.L. Terry et al., Phys. Plasmas 10 (2003) 1739.
[5] A. Zeiler et al., Phys. Plasmas 5 (1998) 2654.
[6] X.Q. Xu et al., Nucl. Fus. 42 (2002) 21.
[7] D.A. D'Ippolito, J.R. Myra, Phys. Plasmas 10 (2003) 4029.
[8] D.H.J. Goodall, J. Nucl. Mater. 111&112 (1982) 11.
[9] J.L. Terry et al., Rev. Sci. Instrum. 75 (2004) 4196.
[10] G.R. McKee et al., Rev. Sci. Instrum. 70 (1999) 913; G.R. McKee et al., Phys. Plasmas 7 (2000) 1870.
[11] J.L. Terry et al., J. Nucl. Mater. 290 (2001) 757.
[12] S.J. Zweben et al., Phys. Plasmas 9 (2002) 1981.
[13] D.P. Stotler et al., J. Nucl. Mater. 313–316 (2003) 1066.
[14] B. Labombard et al., J. Nucl. Mater. 313–316 (2003) 995.